Chapter 13
The Effect of Welding Parameters of Flux Core Arc Welding by Utilizing Robotic Welding

Intan Ramli, Mohd Faizal Abdul Razak, Mohd Zaifulrizal Zainol, and Shaiful Bakri Ismail

13.1 Introduction

Welding is a sculptural or manufacturing process that joins materials. Bonding is a process that occurs at the initial border surface of two pieces of materials, such as metals or thermoplastics. Using high heat, the components can melt together and cool, allowing for fusion (Jun et al. 2014). The welding technique is separated into two broad categories: plastic welding (also known as pressure welding) and fusion welding (also known as non-pressure welding). Fusion welding is a popular welding procedure that includes gas welding, electric arc welding, TIG, MIG, and other welding processes (Rogfel et al. 2021). Pressure welding is another basic type of welding in which the ends of the materials to be joined are brought to a plastic condition and then added by applying pressure as in a welding forge. Welding differs from lower wire-joining temperature methods that do not heat the base metal, such as brazing and soldering.

If necessary, a separate filler material of the same composition as the parent materials is added, and the pool is allowed to solidify and create a well-meant structure.

Welding applications are so diverse and extensive that it would not be misleading to argue that there is no metal industry or engineering division that does not use welding

I. Ramli · M. F. Abdul Razak (✉) · M. Z. Zainol · S. B. Ismail
Universiti Kuala Lumpur Malaysia Institute of Marine Engineering Technology, Jalan Pantai Remis, 32200 Lumut, Perak, Malaysia
e-mail: mfaizalar@unikl.edu.my

M. Z. Zainol
e-mail: mzaifulrizal@unikl.edu.my

S. B. Ismail
e-mail: shaifulbakri@unikl.edu.my

in some form or another, including the automobile, manufacturing, aerospace, and construction industries (Winarto et al. 2018). Mostly used in manufacturing, welding is critical in the shipbuilding industry. Welding is one of the most crucial procedures in shipbuilding. If the welds fail, the entire system fails to protect the ship's hull. This process is carried out by qualified welders and efficiently controlled by quality assurance engineers and classification societies.

Various studies on the interaction between welding parameters and bead geometry are given. Voltage, gas flow rate, wire feed rate, and travel speed are welding parameters that influence the bead geometry (Satyaduttsinh et al. 2014). The quality of the weld is determined by the geometry of the beads. Meanwhile, throughout the welding process, the bead geometry is heavily influenced by the various welding parameters. The welding current is an important welding parameter that influences the bead geometry. The effect of welding current on the bead shape is typically determined by the plate thickness and travel speed. The higher the deposition and penetration rate, the higher the current needed during the welding process. It was discovered that a lower electrode diameter produces smoother material transfer. Meanwhile, the voltage parameter has a strong relationship with the arc length. The size of the weld bead is affected by the arc length. The movement of the arc, on the other hand, is determined by the speed of travel. The lesser the penetration, the slower the travel speed. As a result, it leads to the widen of the weld bead (Vidyut et al. 2008).

Because arc welding is typically done by hand, the quality of the welding is dictated by the welder's ability. A welder with extensive experience is required to provide high-quality weldability. This is due to the welder's ability to directly monitor and select welding parameters during the welding process. To address this issue, robotic welding was introduced. One of the benefits of robotic welding is increased efficiency because the robot can do tasks faster than a human worker (Xu et al. 2017). Furthermore, the quality of welding is more constant and accurate when robot welding is used. Other benefits include faster welding speeds and less waste material due to fewer mistakes made during the welding process. Furthermore, the use of robotic welding can improve the worker's safety, because the robot is outfitted with a variety of safety features that can protect the worker from the welding arc, temperature, and brightness (Kim et al. 2003).

Aside from welding parameters and bead shape, other factors to consider are microstructure, fracture morphology, and micro-hardness. This is typically investigated by an hardness test that will is performed following the welding procedure (Winarto et al. 2018). The goal of the hardness test is to provide two critical indications following the welding procedure. The welding material's strength and microstructure are important considerations. Vickers hardness is a technique for determining welds and HAZs. Loads ranging from 1 to 100 kg can be used to create the diamond indentation. The greater the load, the greater the impact of the diamond on the steel sheet. The goal of having a hardness test for welding is to analyze the hardness of the metal and determine the material tensile strength, as well as to confirm that the welded metal meets or surpasses the original metal's strength requirement.

Table 13.1 Welding parameter

Sample no	Travel speed (mm/s)	Weaving parameter (mm)	Voltage (V)	Current (A)
1	1	0.2	22	130
2	2	0.2	22	130
3	3	0.2	22	130
4	1	0.4	22	130
5	2	0.4	22	130
6	3	0.4	22	130
7	1	0.6	22	130
8	2	0.6	22	130
9	3	0.6	22	130

13.2   Methodology

There are three processes involved in these parts namely the sample cutting process, robotic arm welding, microstructure testing, and hardness testing. The material used in this experiment is the low carbon steel AWS A36 using flux core arc welding (FCAW). The material plate is cut into 18 pieces using a swing beam Guillotine Shear device (SB3006) at UniKL MIMET.

13.2.1   Robotic Arm Welding Setting

A robotic welding arm is an automated welding process, which makes it easy for a welder to get the specific measurement and also can reduce the period for any work project. The setting used for the experiment is as follow; firstly, switch on the main power and then set up the parameter such as current, voltage, travel speed, and weaving parameter as shown in Table 13.1. Next, after setting up all the parameters such as current, voltage, travel speed, and weaving parameter as shown in Table 13.1. Next, after setting up all the parameters then turn on the robotic arm and run the material plates in T-joint configuration. In total a number of specimens was obtained.

13.2.2   Experimental Preparation

In this experiment, after using the robotic arm, all the specimens need to be cut into 1 in. stripes using a semi-automatic horizontal band saw. After the cutting process for each specimen, next polish the selected surface to all the material plated using sandpaper GRIT 800, 1000, and 2000 until mirror look is achieved using a polishing machine (Ghalib et al. 2012). This experiment is conducted at STRIDE in Tentera

Laut Diraja Malaysia (TLDM), Lumut. The process for etching the specimen was done using ferric chloride. Firstly, pour some itching liquid in the petri dish and then put the specimen in the petri dish and wait 1 min or 1 min 30 s (Liu et al. 2019). Then, take out the specimen and rinse it with plain water. After the rinse, use the air gun and blower to ensure there is no etching liquid in the welding gap because it can make the specimen easily corroded.

A stereo microscope is a type of optical microscope that offers a three-dimensional vision of a specimen for the consumer to see. The stereomicroscope differs from the compound light microscope by having different objective lenses and oculars, otherwise referred to as a dissecting microscope or a stereo zoom microscope. For each eye, this results in two autonomous optical paths. The multiple angling views for the left and right eyes provides three-dimensional visuals. Compared to the transmitted light that is used by compound light microscopes, stereo microscopes use reflected light from the object being studied. The magnification varies between 7.5 to 75x. With these tools, opaque, thick solid objects are ideal for studying.

13.2.3 Analysis Preparation

This analysis also is conducted at STRIDE (TLDM) using a stereomicroscope to measure the direction bead height, bead width and throat for penetration after etching. Figure 13.1 shows the nine specimens and the stereo microscope that that is used for this analysis. Next, put one specimen on the stereo microscope, adjust the light and distance to get the actual penetration required. For the light, we did not use the support light because it will disturb the size of the image. It also shows the image on the monitor after putting the specimen on a stereomicroscope. This analysis is continued until finish all the specimens. Lastly, collect all the data and make a comparison of the results obtained.

13.2.4 Hardness Test

This method provides important indication after the welding process. There are three type of hardness test namely the Vickers test, Brinell test and Rockwell test as shown in Fig. 13.2. For this experiment, we used the Vickers test. This technique can be used to measure weld and HAZs. The load that is applied in this experiment 98.1 N because of the Vickers HV10. In calculation it has two diagonals, d1 and d2 are measured, averaged and the surface area is calculated and then divided by the load applied.
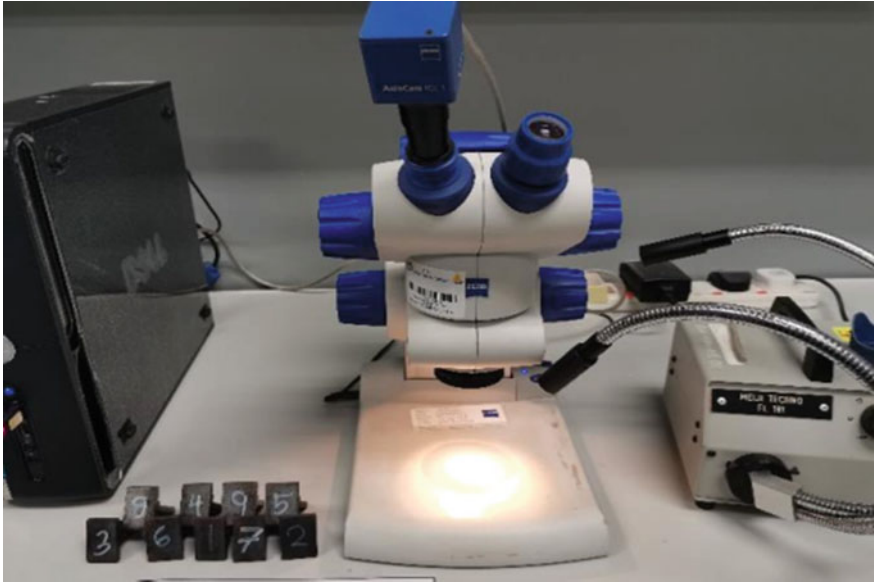
Fig. 13.1 The stereomicroscope

Fig. 13.2 Universal hardness test

13.3 Results and Discussion

The welding is executed using a robotic arm with different weaving parameters and travel speed. The bead geometry is the most important feature in the welding process, especially for automatic systems. In the bead geometry, width, height, and throat are needed in the welding process. There are two testing procedures that were performed in order to analyze the effect of welding parameter on the bead geometry which are microstructure testing and hardness testing (Qing et al. 2021).

13.3.1 Microstructure Testing

This microstructure testing is carried out by measuring the penetration of specimens used in this experiment with a stereomicroscope. Table 13.2 shows the dimensions after using the stereomicroscope on all of the specimens in millimeters.

Figure 13.3 shows the graph of travel speed versus bead geometry. The travel speed start from 1 mm/s, 2 mm/s and 3 mm/s where we can see that with increasing the travel speed, the trend line of bead height, bead width and throat are declining. This is due to the fact that rate of deposition is decreasing when the travel speed is increased and the heat transfer amount is decreasing (Rogfel et al. 2021).

Figure 13.4 indicates that the weaving parameter has a direct effect on the bead geometry profile but from the result does not show a direct correlation for the bead height and throat result (Vidyut et al. 2008). Only bead width shows the direct correlation on weaving parameter to the bead geometry result (Winarto et al. 2018). By applying the same welding parameter set but different weaving value, the data show as the figure above. A weaving value of 0.6 mm shows the highest effect to all the bead geometry, bead height, bead width and throat. The maximum value measured for the bead height is 1.72 mm, for the bead width 1.44 mm and for the throat 1.49 mm. The lowest measurement is for the weaving parameter with a value

Table 13.2 Bead geometry and hardness testing value

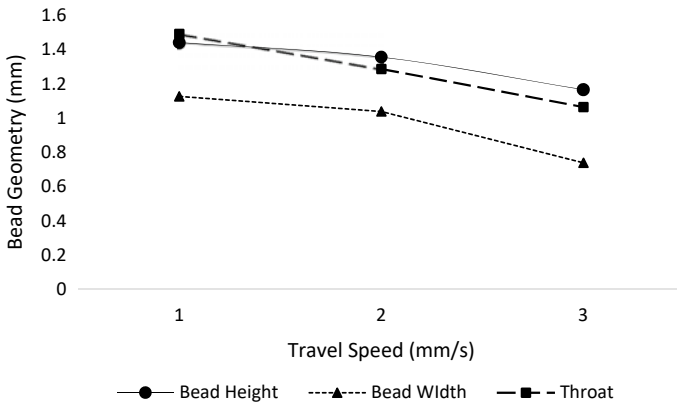| Sample no	High (mm)	Width (mm)	Throat (mm)	HV (kgf/mm^2)
1	1.44144	1.12738	1.49158	1514.504778
4	1.21566	1.21089	1.12721	2061.409281
7	1.71522	1.44285	1.40158	2061.409281
2	1.35634	1.03923	1.28693	1756.46708
5	1.39185	1.14904	1.17202	1756.46708
8	1.28055	0.86139	1.09364	1514.504778
3	1.16615	0.73949	1.06486	1756.46708
6	1.13826	0.97589	1.23427	1514.504778
9	1.0764	0.82891	1.13185	1514.504778

Fig. 13.3 Travel speed versus bead geometry

of 0.4 mm, which affected the bead height and throat only. The value measured is 1.22 mm for bead height and 1.12 mm for the throat value.

Figure 13.5 shows the graph for hardness versus travel speed. The graph shows the result of hv is inclining when the travel speed is increased. The maximum value measured is 2061.41 kgf/mm^2 for a travel speed value is at 0.6 mm/s while the minimum value hv is 1514.50 kgf/mm^2 when the value of travel speed is at 0.2 mm/s. This shows that by increasing the travel speed, the value of hv is directly affected to the travel speed (Winarto et al. 2018).
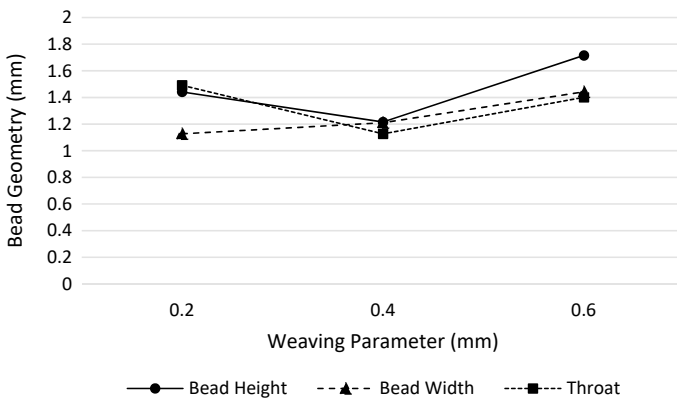

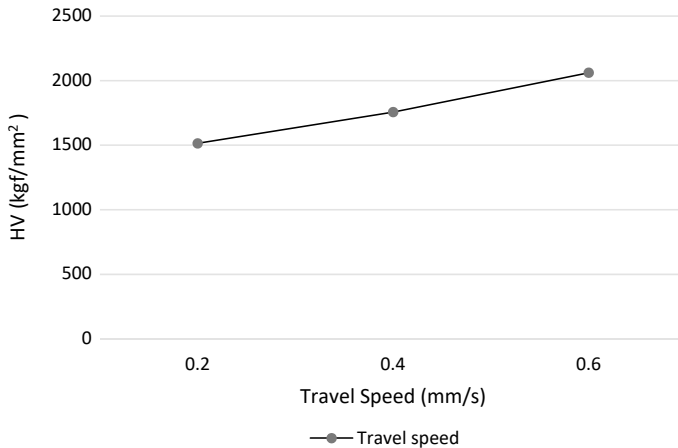**Fig. 13.4** Weaving parameter versus bead geometry

Fig. 13.5 Hardness test versus travel speed

13.4 Conclusion

The objective of this work has been achieved it objective that is to analyze the effect of welding parameter on the bead geometry by using a robotic arm and to identify the hardness of the material after welding by the robotic arm.

References

Ghalib T, Mohamad YY, Sunhaji KA, Yupiter HPM, Bukhari AJ (2012) Predicting the GMAW 3F T-fillet geometry and its welding parameter. Procedia Eng 41:1794–1799

Jun X, Guangjun Z, Jianwen H, Lin W (2014) Bead geometry prediction for robotic GMAW-based rapid manufacturing through a neural network and a second-order regression analysis. J Intell Manuf 25:157–163

Kim IS, Son JS, Kim IG, Kim JY, Kim OS (2003) A study on relationship between process variables and bead penetration for robotic CO2 arc welding. J Mater Process Technol 136:139–145

Liu Q, Song J, Hao P (2019) Automatic reading and writing model of welding parameters predicted based on PSO-RFR. IEEE Xplore 387–391

Qing S, Fuxing T, Kai L, Tatsuo Y, Guikai G (2021) Multi-objective optimization of MIG welding and preheat parameters for 6061–T6 Al alloy T-joints using artificial neural networks based on FEM. MDPI Coatings 11:1–20

Rogfel TM, Guillermo AB, Alysson MAS, Sadek CAA (2021) Analysis of GMAW process with deep learning and machine learning techniques. J Manuf Process 62:695–703

Satyaduttsinh PC, Jayesh VD, Tushar MP (2014) A Review on optimization of MIG welding parameters using Taguchi. Int J Latest Eng Manag Res 4(1):16–21

Vidyut D, Dilip KP, Datta GL (2008) Prediction of weld bead profile using neural networks. ICS 1:581–586

Winarto W, Herry O, Eddy SS (2018) Microstructure and hardness properties of butt and fillet GMAW welded joints on HY80 high strength steel plate. AIP Conf Proc 060020:1–7

Xu Y, Lv N, Fang G, Du S, Zhao W, Ye Z, Chen S (2017) Welding seam tracking in robotic gas metal arc welding. J Mater Process Technol 248:18–30